DOI: http://dx.doi.org/10.4314/star.v3i2.13
ISSN: 2226-7522(Print) and 2305-3372 (Online)
Science, Technology and Arts Research Journal
Sci. Technol. Arts Res. J., April-June 2014, 3(2): 93-102
Journal Homepage: http://www.starjournal.org/

Original Research

Photo-catalytic Removal of Methyl Orange Dye by Polyaniline Modified ZnO using Visible Radiation

Melaku Wondwossen[1]*, Yadav OP[2] and Kebede Tesfahun[3]

[1]Department of Chemistry, Collage of Natural and Computational Sciences, Mizan-Tepi University, Tepi Campus, Post Box No: 121,Tepi, Ethiopia

[2,3]Department of Chemistry, Natural and Computational Sciences, Haramaya University, Post Box No: 203, Dire Dawa, Ethiopia.

Abstract

Polyaniline modified zinc oxide (PANI/ZnO) nanocomposite was synthesized by in-situ polymerization process. The as-synthesized nano-ZnO, PANI and PANI/ZnO nanocomposite were characterized by X-ray diffraction (XRD), FT-IR, and UV-Vis spectroscopy. The UV–visible spectroscopy studies showed that the absorption peak for PANI/ZnO nanocomposite has a red shift toward visible wavelengths compared with the ZnO nanoparticles and PANI. Photocatalytic efficiency of PANI/ZnO nanocomposite was investigated for the degradation of methyl orange (MeO) dye as a model organic compound under Visible light irradiation. The photocatalytic activities of ZnO, PANI and PANI/ZnO nanocomposite were studied. The results showed that ZnO/PANI nanocomposite had greater photocatalytic activity than ZnO nanoparticles and PANI under visible light irradiation. According to these results, application of PANI as a shell on the surface of ZnO nanoparticles causes the enhanced photocatalytic activity of the PANI/ZnO nanocomposite. Influence of some operational parameters such as: amount of photocatalyst, pH of solution, and MeO dye initial concentration on the photodegradation reaction rate was investigated. The optimum values of pH and catalyst dose found to be 6 and 1.50 gmL^{-1} respectively. It was demonstrated that the photocatalytic degradation of MeO follows pseudo first-order kinetics. The PANI/ZnO nanocomposite photocatalysts have good photocatalytic stability and can be reused three times with only gradual loss of activity. Thus, the PANI/ZnO nanocomposites are efficient photocatalytic materials for degrading contaminated colored wastewater for reuse in textile industries under mild conditions.

Article Information

Article History:

Received : 20-03-2014

Revised : 29-05-2014

Accepted : 11-06-2014

Keywords:

PANI/ZnO Nanocomposite

Methyl orange

Visible light

photo-catalysis

Degradation rate constant

***Corresponding Author:**

Melaku Wondwossen

E-mail:

wondosenmelaku@gmail.com

INTRODUCTION

Industries produce a large amount of organic contaminants including dyes which are toxic and non biodegradable. The presence of these contaminants has caused severe environmental pollution problems by releasing toxic and potential carcinogenic substances into the aqueous phase (Kansal *et al*., 2007 and Rashcd, 2007). Contaminants which widely encountered in water are: dyes, chlorinated hydrocarbons, phenol derivative, insecticides, pesticides and pharmaceutical formulations (Doong *et al*., 2001 and Hilal *et al*., 2007).

Various chemical and physical processes such as adsorption, air stirring, flocculation, reverse osmosis and ultra filtration can be used for water purification. But, these techniques are non-destructive and a new type of pollution will arise which needs further treatment (Neppolian *et al*., 2002). Recently, photo catalytic reactions induced by illumination of semiconductors in suspension has been shown to be one of the most promising processes for the wastewater treatment due to its advantages over the traditional techniques, since they provide an interface with an aqueous medium and induce an advanced oxidation process (AOPs), no formation of polycyclic products, oxidation of pollutants in the ppb range (Dai *et al*., 2007). AOPs are based on generation of reactive species such as hydroxyl radicals obtained by the reaction of holes with surface hydroxyl or water and their attachment to organic compound that oxidize a broad range of pollutants efficiently. AOPs include photo-catalysis systems such as combination of semiconductors with light and semiconductor with oxidant (Doong *et al*., 2001 and Kansal *et al*., 2007). Many different semiconductor materials, such as TiO_2, ZnO, ZrO_2, SrO_2, Fe_2O_3, CdS, ZnS have been used to photo-degrade different pollutants (Neppolian *et al*., 2002). Among these, TiO_2 and ZnO are known to be the best photo-catalysts for the degradation of several environmental contaminants (Doong *et al*., 2001 and Neppolian *et al*., 2002).

ZnO has been used to photo-degrade water contaminants in the UV region, but to a much lesser extent than TiO_2. ZnO has comparable band gap (3.34

eV) to that of TiO_2 (3.2 eV). However, the greatest advantage of ZnO is that it absorbs large fraction of solar UV light than TiO_2 does (Kansal *et al*., 2007). TiO_2 can utilize only about 3.0% of the solar light reaching the earth surface for decomposition of organic compounds (Chen *et al*., 2005). The efficient use of sun light became an appealing challenge for developing photoccatalysts (Hilal *et al*., 2007 and Bessekhouad *et al*., 2004). One approach to solve the above problems is to sensitize TiO_2 and ZnO by using narrow band gap semi-conductors with higher conduction band. Some investigations indicated that, the combination of a narrow band gap semiconductor with another with broad band gap results in a better separation of the charge carrier and a quicker transfer of photogenerated electrons in comparison with the single semiconductor material (Georgieva *et al*., 2007). For example, CdS with band gap energy of 2.41 eV is considered to be one of the many sensitizers used for large band-gap semiconductor (Chen and Jie, 2007). This is due to the ideal position of its conduction and valence band edges. CdS alone however, may show lower photocatalytic activity because of rapid electron hole pair recombination rates. Studies have proven that with the appropriate particle interaction, CdS/ZnO nanocomposites can efficiently decompose organic compounds such as phenol, methyl orange and methylene blue under visible irradiation.

Another approach, many researches focused on increasing degradation rate of pollutants by combining inorganic materials with conductive polymers to realize synergetic and complementary behaviors between the polymer and inorganic materials (Sharma *et al*., 2009). Many conducting polymers are known as good hole conducting materials (Shaheen *et al*., 2001). These conductive polymers act as a stabilizer or surface capping agents when combined with metals or semiconductor nanoparticles (Mbhele *et al*., 2003, Karim *et al*., 2006 and Khanna *et al*., 2004). Conducting polyaniline (PANI) is one of the promising studied polymer, due to its high conductivity, simple synthesis procedure, good environmental stability (Gustafsson *et al*., 1992). There are several reports focused on increasing ultraviolet emission and photocatalytic activity of ZnO nanostructures combined with polyaniline conductive polymer (Ameen *et al*., 2011 and Chang *et al*., 2007).

In addition, ZnO has been frequently considered as an alternative to TiO_2 for photocatalytic applications, since it shows similar activity in certain conditions. However, it suffers from anodic photocorrosion, differently to TiO_2, and ZnO is soluble in strong acids and alkalis, which limits the pH range in which it can be used. The photocatalytic activity of semiconductor depends upon the crystallinity, surface area and particle morphology. Among these factors, crystallinity and surface area which depend on the method of preparation are regarded as important factors for determining photocatalysis (Parida *et al.,* 2006). Inorganic nanoparticles are also very easy to agglomerate in media. To prevent agglomeration of nanoparticles in mediums, their combination with polymers is usually accomplished by surface modification. It can significantly enhance the stability of nanoparticles dispersing in polymer solvents by increasing the affinity of the surface for organic substances (Kim *et al.,* 2005). In the present work, the efficiency of the photocatalytic destruction of methyl orange using visible light and polyaniline modified ZnO nanocomposite was studied. Specifically, the effect of irradiation time, concentration of PANI/ZnO photocatalyst and MeO, and pH of the solution were examined.

MATERIALS AND METHODS

Chemicals

In present study, zinc chloride (assay $\geq$ 98%), aniline (assay $\geq$ 99%), ammoniumperoxydisulfate (APS) (assay $\geq$ 98%), methyl orange, sodium hydroxide (assay 99%), hydrochloric acid (assay $\geq$ 37%) and 2-propanol (assay $\geq$ 99.8%). All chemicals were analytical grade. Double distilled water was used for preparation of various solutions.

Synthesis of Photocatalyst (ZnO Nanoparticles)

ZnO nanoparticle synthesis method was adapted from (Kathirvelu *et al.,* 2009). 5.5gm of $ZnCl_2$ was dissolved in 200 ml of water at 90^0C in a beaker and 16 ml of 5M NaOH aqueous solution was added dropwise to the $ZnCl_2$ solution with a gentle stirring over a period of 10 minutes. The particles were separated from the supernatant by sedimentation. The supernatant solution was discarded and the solid residue was washed five times with distilled water to remove NaCl. The particles were peptized with 2-propanol for 10 minutes at room temperature. Then the particles were collected by centrifugation at 6,000 rpm for 15 minutes and then washed three times with distilled water. Finally, the product was thermally treated at 250^0C for 5 hours to form ZnO powder.

Synthesis of Photocatalyst (Polyaniline Modified ZnO (PANI/ZnO) Composite)

A typical oxidative polymerization method was adopted for polymerization of aniline in the presence of ZnO nanoparticles (Olad and Nosrati, 2011). 0.9313 g of ZnO powder was added into 20 mL aqueous solution of 0.01 mol aniline monomer and 0.01 mol hydrochloric acid. 0.01 mol APS was dissolved in a 15 ml distilled water and added dropwise to the mixture of ZnO and aniline with stirring in an ice bath. Polymerization proceeded for 5.5 hours. The composite of PANI modified ZnO was obtained as precipitate. The precipitate was isolated by filtration, washed with distilled water and ethanol several times, and dried at 50^0C. Pure PANI was also synthesized, by using an identical method but without using ZnO.

Characterization of Synthesized Photocatalysts

The products were characterized by X-ray diffraction (XRD) on West Germany X-ray diffractometer (XRD) equipped with a Cu target for generating a Cu Kα radiation (wavelength 1.5406 A°) as the X-ray source. The measurements were made at room temperature and the accelerating voltage and the applied current were 40 kV, 30 mA respectively. The instrument was operated under step scan type with step time and degree (2θ) of 1s and 0.020°, respectively, ove 4° to 64°. The UV–visible spectra of photocatalysts were measured using Perkin Elmer sectrophotometer (model; SANYO SP65) to evaluate their photoactivation wavelengths. FTIR spectra with KBr pellets were recorded in the range 4000 to 400 cm^{-1} to infer the interaction between ZnO and molecular chains of PANI in the PANI/ ZnO composite.

Determination of Point of Zero Charge (PZC)

Point of zero charge (pzc) of PANI/ZnO composite was determined using the method described by Rao *et al*., (2011). The adsorbent (100 mg) suspension was prepared in 50 ml solution of 10^{-3} M $NaNO_3$ and adjusted

to various pH values using dilute NaOH and HNO_3 solutions. Allowing 60 min for equilibration, the initial pH value was measured. Then 1.0 g of $NaNO_3$ is added to each aliquot to bring final electrolyte concentration to 0.45 M. Final pH was measured after 60 minutes agitation. A plot of $pH_{final-initial}$ versus pH_{final} was drawn.

MeO Degradation Studies

Photocatalytic degradation of methyl orange (MeO) was carried out using a reactor (figure 1). Photocatalytic degradation experiments were carried out at room temperature (25^0C) at night to avoid sunlight penetration. 100 mL of dye solution 10 mgL^{-1} was mixed with 150 mg of PANI/ZnO composite. The suspension was constantly stirred for 30 min in dark before irradiation to reach absorption equilibrium of PANI/ZnO with dye solution. During irradiation, the reaction mixture was maintained under magnetic stirring to achieve a homogeneous suspension, to promote the adsorption of dye on the surface of the photocatalyst (Xu *et al*., 1998). At each 20 minute interval, 10 mL dye solution was collected and centrifuged at 5000 rpm for 10 min and filtered. Dye concentration was determined using UV/Visible spectrophotometer at the λ_{max} of MeO dye (460 nm). The photodegradation efficiency (% degradation) was calculated using Eq.4.

$$\%\ \textbf{Degradation} = \frac{\mathbf{A_0 - A_t}}{\mathbf{A_0}}\ \mathbf{x\ 10} = \left(\mathbf{1} - \frac{\mathbf{A_t}}{\mathbf{A_0}}\right)\mathbf{x100}$$

Where A_0 is absorbance of MeO dye in solution at the initial stage, A is the absorbance at time (t).

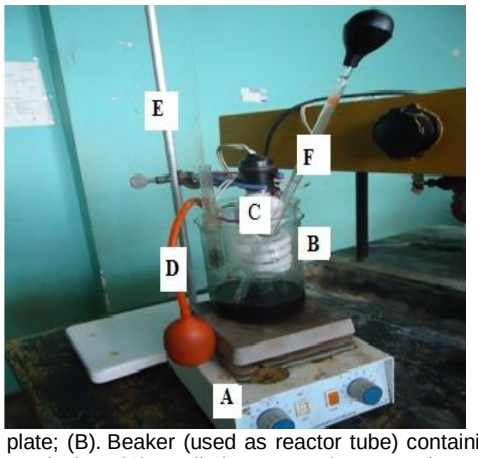

(A). Hot plate; (B). Beaker (used as reactor tube) containing the reactants and stirrer;(C). Radiation source (Tungsten lamp, 40W) (D). Purging pump to inlet air to the solution; (E). Stand to hold the lamp and (F). Sample collecting pipette

Figure 1: Photocatalytic reactor.

Kinetic Studies of Photocatalytic Degradation of MeO

The kinetics of the photolytic degradations of methyl orange solutions was investigated using initial concentrations of dye in the range 10 - 40 mgL^{-1}, in the same operating conditions. The graph was plotted between $\ln C_o/C_t$ as a function of time (t). Where, C_o is the initial concentrations of dye and C_t is concentration of dyes at time t. From the slope of the plot, the rate of the photocatalytic degradation of MeO was determined.

RESULTS AND DISCUSSION

X-ray Diffraction (XRD) Analysis

XRD patterns of PANI, PANI/ZnO and ZnO are shown in figure 2. In the XRD pattern of ZnO, the observed peaks at $2\theta = 32^0$, 34.5^0, 36.4^0, 47.6^0, 56.5^0, and 63^0 correspond to planes (100),(002), (101),(102),(110) and (103), respectively, suggesting hexagonal zincite crystal structure for ZnO (Kathirrvelu *et al.,* 2009). The broadened and intense XRD peaks indicate the formation of nanosize ZnO particles. Absence of extra peaks in the XRD indicates that there are no impurities present in the sample. The average particle size of ZnO, considering the most intense peak of (101) is 33.87 nm obtained using Debye- Scherrer formula (Zheng and Wu, 2009): $D = k\lambda/\beta Cos\theta$ Where D is the crystallite size in nm, K is the shape factor constant and taken as 0.94, β is the full width at half maximum (FWHM) in radians, λ is the wavelength (0.15406 nm) of the X-ray for Cu target K_α radiation and θ is diffraction angle. The XRD pattern of PANI in figure 3, two weak peaks are observed at 2θ=20° and 2θ=25°. The peak at 2θ =20° represents the characteristic distance between the ring planes of benzene rings in adjacent chains or the close contact inter-chain distance (Pouget *et al*., 1995). The peak centered at 2θ=25° may be assigned to the scattering from PANI chains at interplanar spacing (Feng *et al*., 2000 and Min *et al*., 2007) and very low intensity of the observed peak indicates that the PANI has amorphous structure with low crystallinity. The XRD pattern of the PANI/ZnO nanocomposite (in figure 4) include the characteristic peaks of both PANI and ZnO, which confirms the formation of nanocomposite with lower crystallinity.

FT-IR Analysis

FTIR spectrum is the feature of a particular compound that gives the information about its functional groups, molecular geometry and inter/intramolecular interactions. Figure 5 shows the FTIR spectra of ZnO nanoparticles. The absorption peak near 486 cm^{-1} is due to stretching vibrations of Zn-O bonds. The peaks at 3435 cm^{-1} and 2920 cm^{-1} indicate the presence of OH and C=O residues respectively, probably due to atmospheric moisture and CO_2 respectively (Silva and Zaniquelli, 2002). Figure 6(a) shows the FTIR spectra of pure PANI. The caracterstics peaks are 1575 cm^{-1} due to C=C stretching mode of the quinoid rings, 1497 cm^{-1} due to C=C stretching mode of benzenoid rings, 1298 cm^{-1} due to C–N stretching mode and 1151 cm^{-1} due to N=Q=N, where Q represents the quionoid ring (Silva and Zaniquelli, 2002). The presence of the benzenoid and quinoid units is evidence of the emeraldine form of PANI. The FTIR spectrum of the PANI/ZnO nanocomposite (Figure 6 b) is the replica of characteristic peaks of PANI. However, the corresponding peaks are shifted to the lower wave numbers, besides their intensities are changed after the ZnO nanoparticles addition. The peaks of the PANI around 1575 cm^{-1}, 1497 cm^{-1}, 1298 cm^{-1} and 1151 cm^{-1} are shifted to 1567 cm^{-1}, 1482 cm^{-1}, 1289 cm^{-1} and 1132 cm^{-1} respectively. These shifts of characteristic peaks of the PANI may be the result of the interactions between the PANI chains and ZnO nanoparticles which affect the electron densities and bond energies of the PANI (Somani *et al.*, 1999 and Niu *et al*., 2003). The shifting to the lower wave numbers shows the increasing the electron density of PANI chains or due to the action of hydrogen bonding between the hydroxyl groups on the surface of ZnO nanoparticles and the amine groups in the PANI molecular chains (He, 2005). Similar observations of shifting of absorption peaks of PANI/ZnO towards lower wavenumber were also reported earlier (He, 2004).

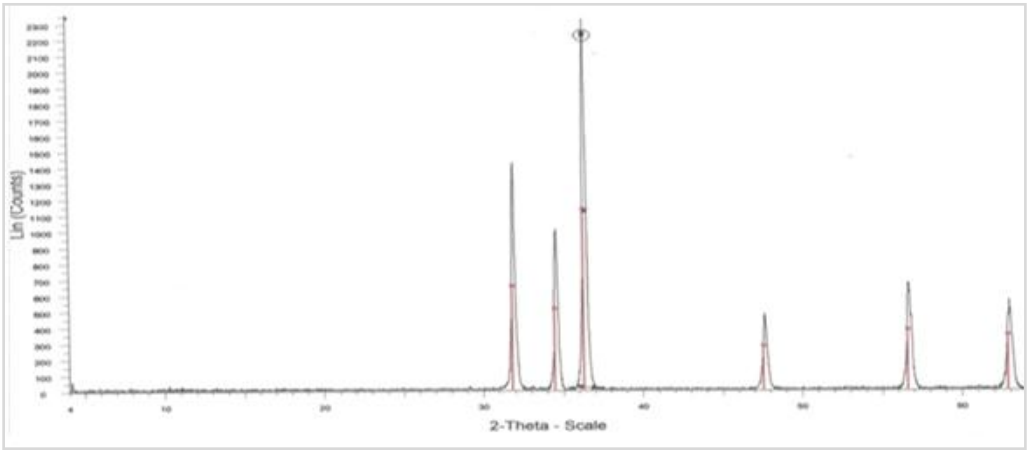

Figure 2: XRD pattern of ZnO nanoparticles

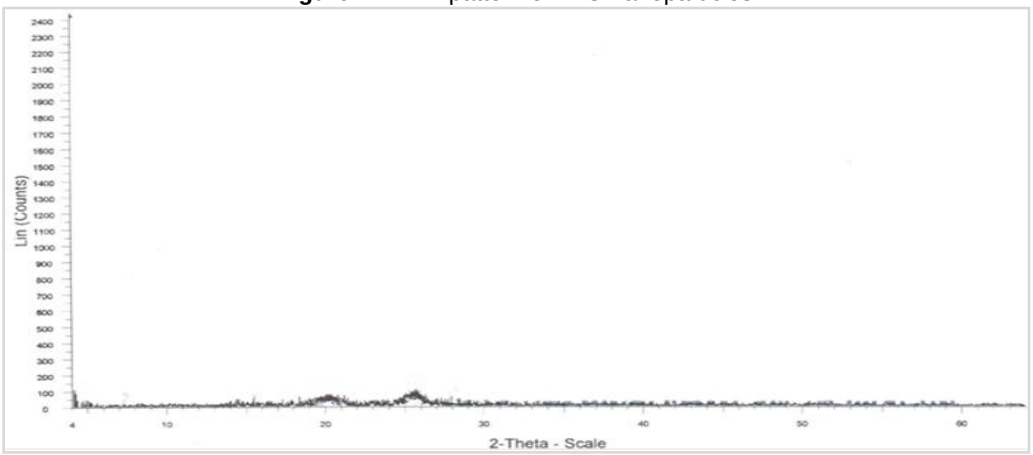

Figure 3: XRD pattern of PANI

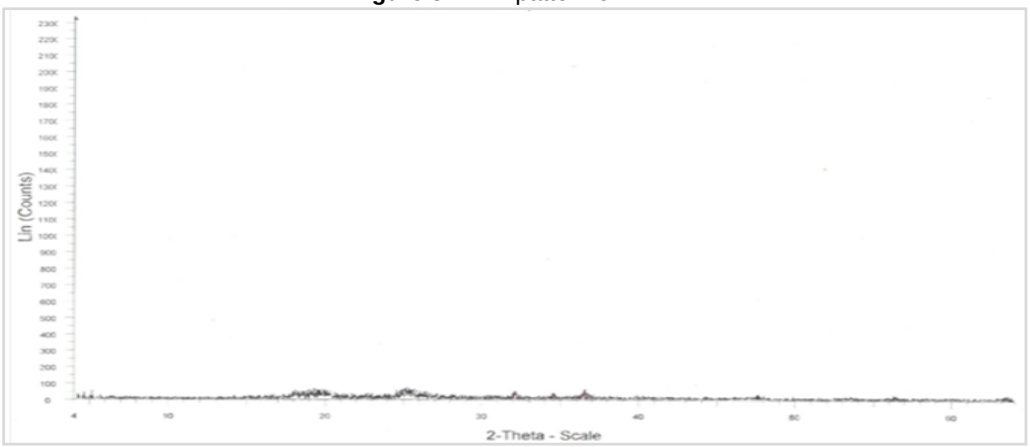

Figure 4: XR D patter of PANI/ZnO nanocomposite

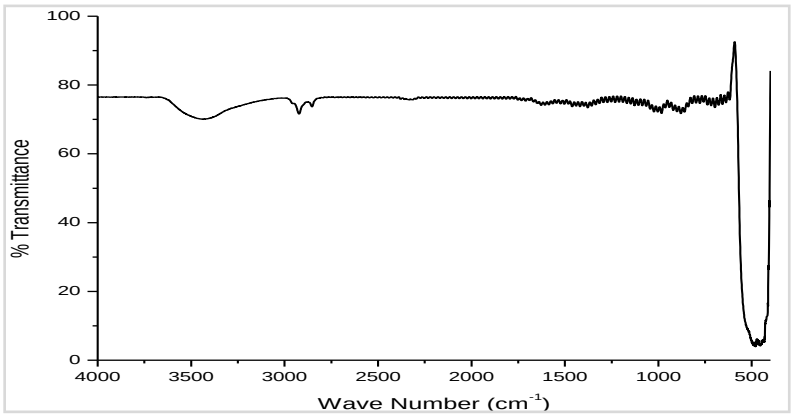

Figure 5: FTIR spectrum of ZnO nanoparticle

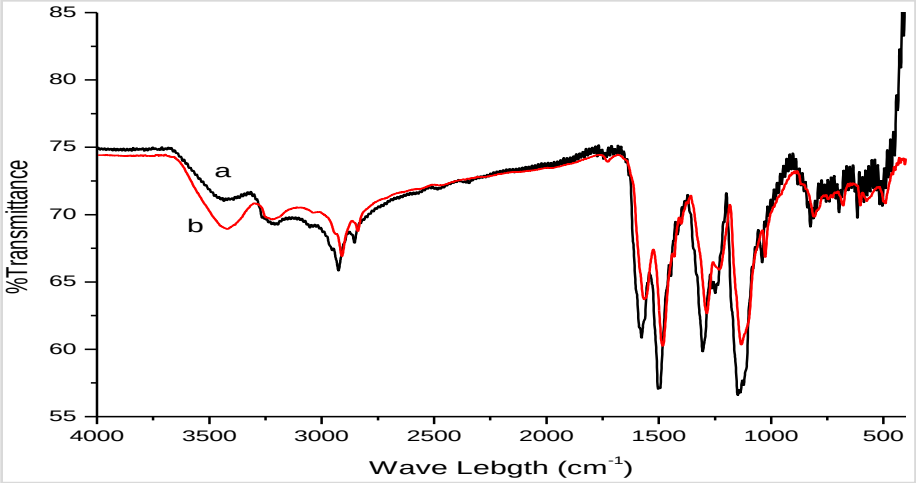

Figure 6: FTIR Spectra of a) the PANI polymer and b) PANI/ZnO nanocomposite

UV-Vis Absorption Spectra

To investigate the effect of combining ZnO nanoparticles with PANI on the spectroscopic absorption of ZnO nanoparticles, the UV–visible absorption spectra of all components were recorded and analyzed. Figure 7 shows the UV–visible spectra of ZnO nanoparticles (a), PANI (b) and PANI/ZnO nanocomposite (c). The absorption spectrum of the ZnO nanoparticles (Figure 7a) presents a sharp absorption peak around 379 nm which is the characteristic single peak of hexagonal ZnO nanoparticles. PANI shows absorption both in UV range as well as in the visible region. As reported previously by some researchers doped forms of PANI shows usually three characteristic absorption bands at 320-360, 400-450 and 740-960 nm (Wang *et al*., 2010). The first absorption band arises from $\pi - \pi^*$ electron transition within benzenoid segments (Sedenkova *et al*., 2008). The second and third absorption bands are related to doping level and formation of polarons (quinoid segments), respectively. Similarly, the PANI has absorption band around 447 nm as shown in figure 7b. In the literature, the absorption peaks of PANI between 700-800 nm was related with the presence of acidic solvents used as medium during polymerization of aniline (Xu *et al*., 2007). The UV–visible spectrum of the PANI/ZnO nanocomposite (figure 7c) has an absorption peak at 471nm, which is red shifted compared with the absorption peaks of pristine PANI (454 nm) and of ZnO nanoparticles (379 nm). This may be because of interactions between PANI chains and ZnO nanoparticles which cause easy charge transfer from PANI to ZnO via hydrogen bonding. Compared with neat ZnO, the absorption of PANI modified ZnO sample increases over the whole range of visible light whereas decreases in the UV range (Olad and Nosrati, 2011). According to these results, the synthesized PANI/ZnO nanocomposite that shows shift of absorption peak in the visible region, it was photoactivated by visible light irradiation compared to ZnO photocatalyst nanoparticles which are photoactivated under harmful UV light irradiation. This may be the main advantage of the PANI/ZnO nanocomposite prepared in this study, which has a special structure which is only photoactivated under visible light irradiation.

The band gap energy (E_g) of photocatalyst was obtained using the equation: $E_g = \frac{1240}{\lambda}$ eV , where E_g is the band gap energy (eV), λ the absorption adge wavelength (nm) (El-Kemary *et al*., 2010). The band gap energy of ZnO and PANI/ZnO composite are 3.27 and 2.73 eV, respectively.

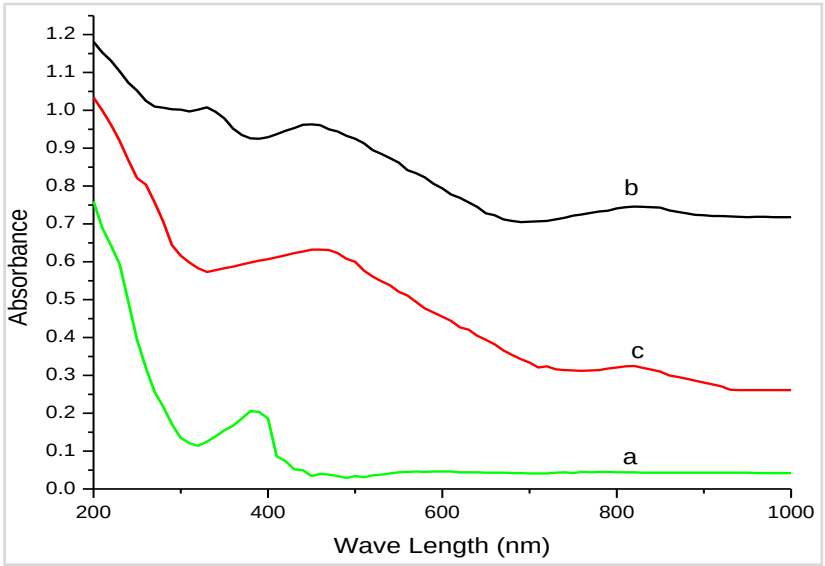

Figure 7: UV–visible spectra of ZnO nanoparticles (a), pristine PANI (b), and PANI/ZnO nanocomposite (c)

Point of Zero Charge (pzc) of PANI/ZnO Nanocomposite

The plot of pH_f versus pH_{f-i} is shown in figure 8. The pH_{zpc} values for adsorbent/ photocatalyst PANI/ZnO nanocomposte is 8.17. This means that the PANI/ZnO nanocomposite has acidic nature below 8.17, basic nature above 8.17 and neutral at pH = 8.17.

Methyle Orange Degradation Studies

Comparision of Photocatalysts

Photocatalytic activity of as-synthesized ZnO nanoparticles, pristine PANI, and PANI/ZnO nanocomposite under visible light irradiation for degradation of MeO dye molecules was evaluated and compared. Figure 9 shows the percentage degradation of MeO dye in solutions with the same dye initial concentration of 10 mg L^{-1} with the same amount (1.50 gm L^{-1}) of different photocatalysts ZnO, pristine PANI, and PANI/ZnO nanocomposite under visible light irradiation. The results shows that, ZnO has negligible photocatalytic activity under visible light irradiation. This is because of the large band gap of ZnO (3.27 eV) that is available only with the UV radiation and cannot be provided by visible light radiation used here. Pristine PANI has photocatalytic activity under visible light irradiation for the degradation of MeO molecules. The degradation or decolorization efficiency of MeO solution under visible light irradiation using pristine PANI and PANI/ZnO nanocomposite were 38% and 81.3% at 2 hours. This may be because in case of PANI/ZnO, there is efficient charge separation of electron and hole pairs in the excited states that prevents recombination of charge pairs for a longer time under visible radiation (Olad and Nosrati, 2011).

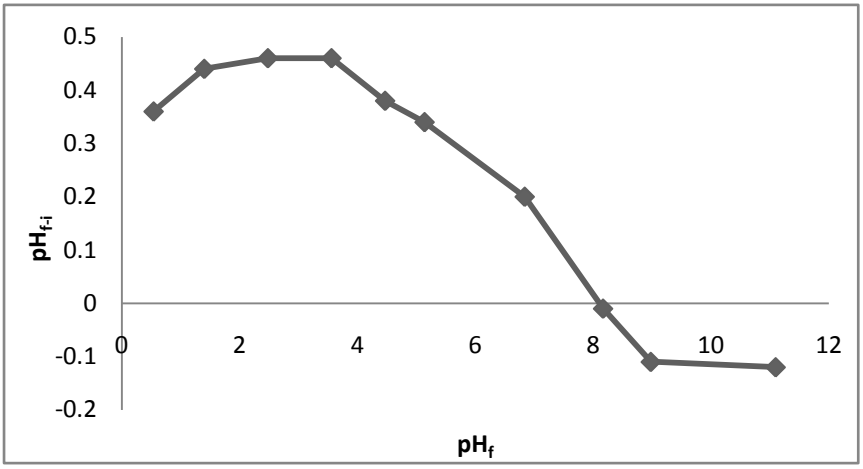

Figure 8: Plot of pH_f versus pH_{f-i} of PANI/ZnO nanocomposite.

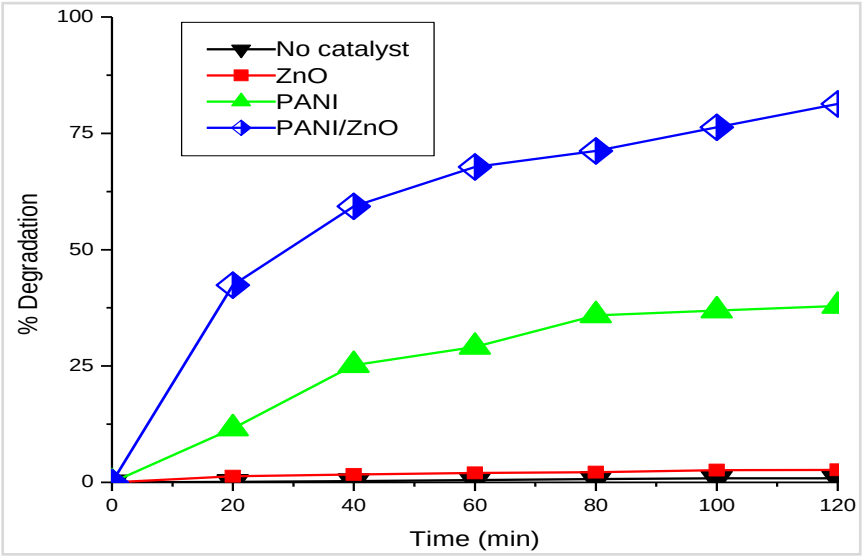

Figure 9: Plots of percentage degradation of MeO as function of time under Visible irradiation using ZnO, PANI and PANI/ZnO photocatalysts (MeO = 10 mgL^{-1}, ZnO, PANI and PANI/ZnO =1.50 gmL^{-1}, pH = 6).

Effect of Irradiation Time

The relationship between the percentage degradation of MeO dye by PANI/ZnO photocatalyst and irradiation time is shown in Figure 9. It is clearly seen that the percentage degradation increases with increasing irradiation time and is 81.3% degradation at 120 minutes using PANI/ZnO photocatalyst.

Effect of Photocatyst (PANI/ZnO) on the Photocatalytic Degradation of MeO Dye

The amount of photocatalyst is one of the main parameters for the degradation of substrate from economical point of view. In order to avoid the use of excess photocatalyst, it is necessary to find out the optimum loading of photocatalyst for efficient removal of

dye (Sakthivel *et al*., 2003). Hence, a series of experiments were carried out to find the optimum amount of the photocatalyst (PANI/ZnO) by varying its amount from 0.50 gL^{-1} to 2.50 gL^{-1}. The percent degradation of dye versus time of degradation by varying the photo catalyst weight is shown in figure 10. To achieve highest photocatalytic reaction rate, the optimum amount of the photocatalyst is found to be 1.50 gL^{-1}. The observed dependence of reaction rate on the amount of photocatalyst can be explained in terms of the availability of active sites at the adsorbent surface and the level of light penetration in the reaction medium (Goncalve *et al*., 1999). Upon increasing the amount of photocatalyst up to 1.50 gL^{-1} percent degradation increases due to the increase in the adsorbent total surface area and thus, the number of active sites, available for the photocatalytic reaction. However, excess photocatalyst, above optimal load, would induce more aggregation (particle–particle interactions) of photocatalyst making a significant fraction of the catalyst inaccessible either to the adsorbing dye or to the radiation (Wong and Chu, 2003).

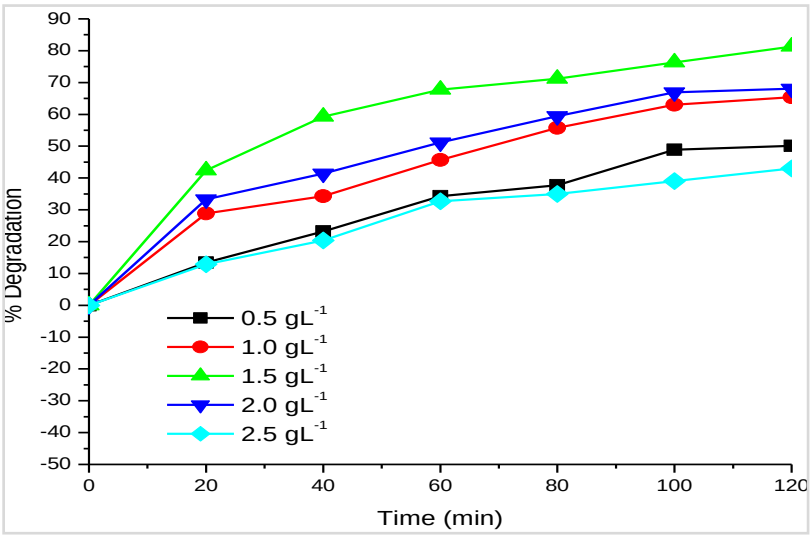

Figure 10: Plot of perecent degradation of MeO versus time by varying the amount of PANI/ZnO photocatalyst (pH = 6, MeO 10 mgL^{-1}, λ_{max} = 460 nm).

Effect of pH

The pH of solutions greatly affects the rate of reaction taking place on semiconductor surfaces due to its influences on surface-charge-properties of the photocatalysts. The effect of pH in the range of pH 3.0 – 11.0 on the photo-catalytic degradation rate of MeO was investigated. Plot of photocatalytic degradation as a function of time is presented in figure 11. The strong effect of pH on the photodegradation efficiency of MeO solution was observed at pH of 6.0. Net charge on the photocatalyst surface is pH dependant. PANI/ZnO photocatalyst has point of zero charge (pzc) at pH = 8.17. Below the pzc the photocatalyst has net charge positive and above the pzc the net charge on it is negative. Lower photocatalytic degradation at a lower pH (than pzc) is due to the less availability of OH^- ions to form highly active $OH^\bullet$ radicals. At higher pH (than pzc) sorption of negatively charged MeO on the similarly charged photocatalyst decreases due to ion-ion repulsion and hence there is less photocatalytic degradation of MeO dye.

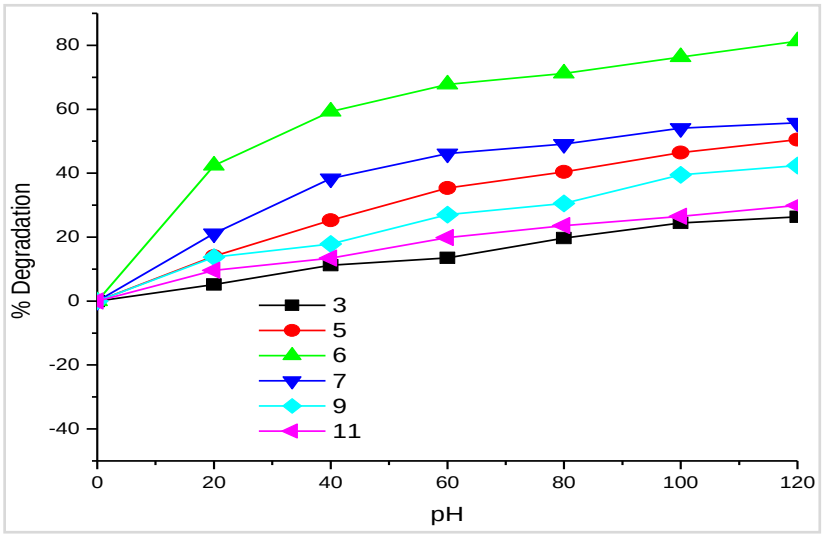

Figure 11: Plots of percent degradation of MeO as function of pH under visible irradiation using PANI/ZnO photocatalyst (MeO = 10 mgL^{-1}, PANI/ZnO =1.50 gL^{-1}, pH = 6, λ_{max} = 460 nm).

Effect of Initial Concentration on the Photocatalytic Degradation of MeO Dye

The effect of the substrate initial concentration on the degradation of MeO dye was studied at different concentrations of dye varying from 10 mg L^{-1} to 50 mg L^{-1} keeping photocatalyst load (1.50 gL^{-1}). Figure 12 shows the percentage degradation of MeO dye in solutions with the same amount of PANI/ZnO photocatalyst (1.50 g L^{-1}). The highest degradation was found to be maximum using 10 mg L^{-1}concentration of MeO. As the dye concentration is increased and the catalyst amount is kept constant, fewer active sites are available per substrate (dye) to interact with. Thus, resulting in decreased rate of photocatalytic degradation (Davis *et al*., 1994, Poulios and Aetopoulou, 1999). Further, at higher dye initial concentration, the approach of the radiation photons to the catalyst surface is hindered and screened off, thereby, reducing the photocatalytic activity in the system (Epling and Lin, 2002; Zhu *et al*., 2000). Moreover, at the higher dye concentration, the number of collisions between dye molecules increases at the cost of required collisions between dye molecules and ·OH radical and therefore, the rate of reaction is retarded (Lodha *et al*., 2008).

Kinetic Study of Dye Photo-catalytic Degradation

The values of $\ln(C_0/C_t)$ as a function of time for different concentration of MeO are shown in figure 13. The linear correlation of the plot of $\ln (C_0/C_t)$ as a function of time suggested that, photocatalytic degradation of MeO dye is a pseudo first-order reaction. The correlation constant for the fitted line was calculated to be R^2 = 0.996, 0.989, 0.993 and 0.982 for MeO concentrations 10, 20, 30 and 40 mgL^{-1} respectively. The rate constants were calculated to be 0.014, 0.01, 0.004 and 0.001.

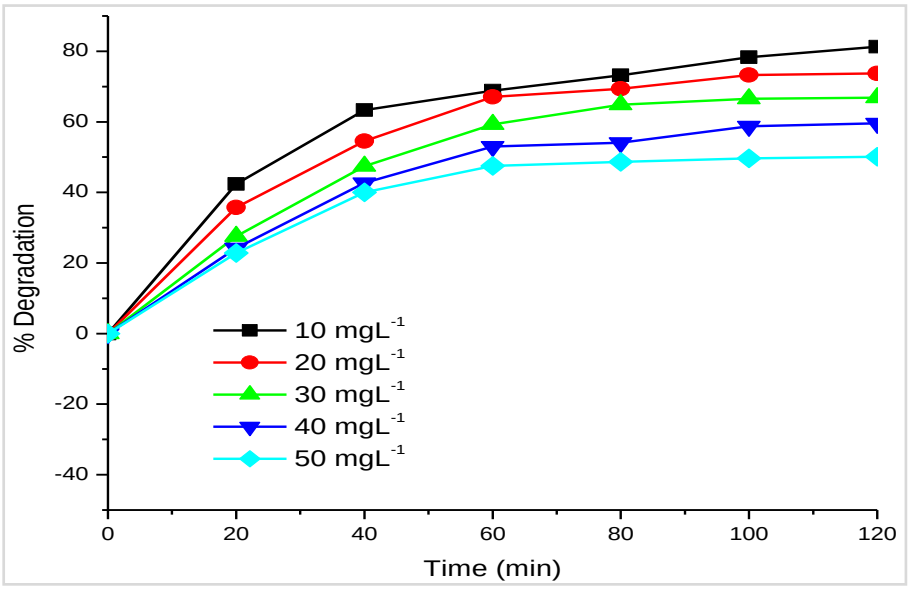

Figure 12: Plots of percentage degradation as function of time under visible light irradiation by keeping the PANI/ZnO photocatalyst cconstant and varying the amount of MeO solution (PANI/ZnO =1.50 gL^{-1}, pH = 6, λ_{max} = 460 nm).

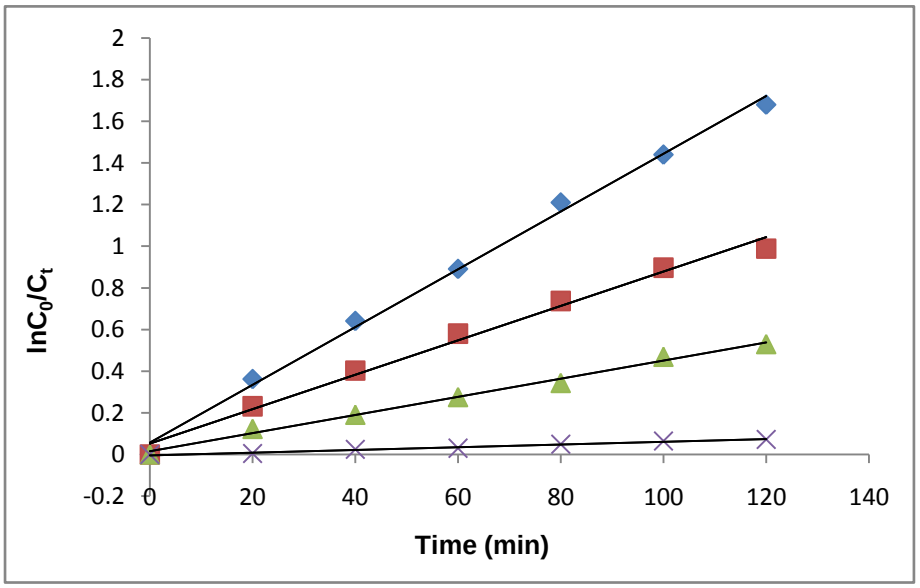

Figure 13: Plot of $\ln(C_0/C_t)$ as a function of time for photocatalyzed degradation of different concentration of MeO dye by PANI/ZnO photocatalys (PANI/ZnO =1.50 gL^{-1}, pH = 6, λ_{max} = 460 nm).

CONCLUSIONS

The PANI polymer and the PANI/ZnO nanocomposites have been successfully prepared via a facile chemical polymerization method. ZnO nanoparticles were successfully coated with PANI through 'in situ' chemical oxidative polymerization of aniline. The results of FTIR and UV-vis. confirm that there is a strong interaction between PANI and ZnO nanoparticles.

The superior photocatalytic effect of the PANI/ZnO nanocomposite is attributed to the synergistic effect of PANI and ZnO which promotes migration efficiency of the photogenerated carriers on the PANI/ZnO interface. The effects of operational parameters such as: amount of photocatalyst, pH of MeO solutions, and dye initial concentrations on the photocatalytic degradation rate of MeO solutions have been investigated. The photodegradation rate initially increases with the increase of catalyst amount up to optimum of PANI/ZnO photocatalyst (1.50 gL^{-1}), above this load the photodegradation rate of MeO solution decreases. The photocatalytic capacity of PANI/ZnO nanocomposite towards degradation of methyl orange solutions also depends on the pH of MeO solutions, and there exists optimum pH (6.0) for maximum degradation of MeO dye. Photocatalytic degradation using polymer-sensitized ZnO composites presents a promising method for addressing environmental pollution. Thus, the PANI/ZnO nanocomposites are efficient photocatalytic materials for degrading contaminated colored wastewater for reuse in textile industries under mild conditions.

ACKNOWLEDGEMENT

I am deeply indebted to my advisors Prof. O. P. Yadav and Dr. Tesfahun Kebede for their invaluable and stimulating interest and unreserved support, most generously given during the course of my study. I pay respect and express indebtedness to them because of their guidance, consistent supervision as well as suggestions at every phase of this thesis work that made it possible to materialize.

REFERENCES

Ameen, S., Akhtar M.S., Kim Y.S., Yang O. and Shin H. (2011). An effective nanocomposite of polyaniline and ZnO: preparation, characterizations, and its photocatalytic activity. *Colloid and Polymer Science* 289: 415-421.

Bessekhouad, Y., Robert D. and Weber J.V. (2004). Bi_2S_3/TiO_2 and CdS /TiO_2 heterojunctions as an available configuration for photo catalytic degradation of organic pollutant. *Journal of Photochemistry and Photobiology A: Chemistry* 163: *569-580.*

Chen, F. and Jie W. (2007). Growth and photoluminescence properties of CdS solid solution semiconductor. *Crystal Research & Technology* 42: 1082- 1086.

Chen, F., Zhigang, X. Li, Zhang J. and Zhao J. (2005). Visible light detoxification by 2, 9, 16, 23-tetracarboxyl phthalocyanine copper modified amorphous titania. *Chemical Physics Letters* 415: 85- 88.

Dai, K., Chen H., Peng T., Ke D., Yi K. (2007). Photo catalytic degradation of methyl orange in aqueous suspension of meso porous Titania Nano particles. *Chemosphere* 69: 1361-1367.

Davis, R.J., Gainer J.L., Neal G.O. and Wu I.W. (1994). Photocatalytic Decolorization of Wastewater Dyes. *Water Environment Research* 66: 50-53.

Doong, R., Chen C., Mathreepala R.A., and Chang S. (2001). The influence of pH and cadium sulfide on the photo catalytic degradation of 2-chloro phenol in titanium dioxide suspensions. *Journal of Veterinary Research* 35: 2873-2880.

El-Kemary, M., El-Shamy H. and El-Mehasseb I. (2010). Photocatalytic degradation of ciprofloxacin drug in water using ZnO nanoparticles. *Journal of Luminescence* 130:2327–2331.

Epling, G.A. and Lin C. (2002). Photoassisted bleaching of dyes utilizing TiO_2 and visible light. *Chemosphere* 46: *56*1- 570.

Feng, W., Sun E., Fujii A., Wu H., Nihara K., Yoshino K. (2000). Synthesis and Characterization of Photo-conducting Polyaniline-TiO2 Nanocomposite. *Bulletin of the Chemical Society of Japan* 73: 2627-2633.

Georgieva J, Armyanov S. and Valova E. (2007). Enhanced photocatalytic activity of electrosynthesised tungsten trioxidetitanium dioxide bi-layer coatings under ultraviolet and visible light illumination. *Electrochemistry Communications* 9: 365-370.

Goncalves, M.S.T., Oliveira-Campos A.M.F., Pinto E.M.M.S., Plasencia P.M.S. and Queiroz M.J.R.P. (1999). Photochemical Treatment of Solutions of Azo Dyes Containing TiO_2. *Chemosphere* 39:781-786.

Gustafsson, G., Cao Y., Treacy G.M., Klavetter F., Colaneri N. and Heeger A. (1992). Flexible light emittind diods made from soluble conducting polymers. *Nature* 357: 477-479.

He, Y. (2004). Preparation of polyaniline/nano-ZnO composites via a novel. Pickering emulsion route. *Powder Technology* 147: 59.

He, Y. (2005). ZnO composite fibers. *Applied Surface Science* 249: 1.

Hilal, H.S., majiad L.Z., Zaatar N. and El-Hamouz A. (2007). Dye-effect in TiO_2 catalyzed contaminant photo degradation: Sensitization vss.Charge transfer form alism. *Solid State Sciences* 9: 9-15.

Kansal, S.K., Singh, M. and Sud, D. (2007). Studies on photo- degradation of two commercial dyes in aqueous phase using different photo catalysts. *Journal of Hazardous Materials* 141: *58* 1-590.

Karim, M.R., Lee C.J., Park Y.T. and Lee M.S. (2006). Synthesis and characterization of conducting polythiophene/carbon nanotubes composites. *Journal of Polymer Chemistry* 14: 5283-5290.

Kathirvelu, S., D'Souza L.and Dhurai B. (2009). UV protection finishing of textiles using ZnO nanoparticles. *Indian Journal of Fibre and Textile Research* 34: 267-273.

Khanna, P.K., Lonker S., Subbarao V.S. and Jun K.W. (2004). Polyaniline/CdS nanocomposite from organo-metallic cadmium precursor. *Materials Chemistry and Physics* 87: 49-52.

Kim, S., Kim E., Kim S. and Kim W. (2005). Surface modification of silica nanoparticles by UV-induced graft polymerization of methyl methacrylate. *Journal of Colloid and Interface Science* 292(1): 93–98.

Lodha S., Vaya D., Ameta R. and Punjabi P. (2008). Photocatalytic degradation of Phenol Red using complexes of some transition metals and hydrogen peroxide. *Journal of the Serbian Chemical Society* 73: 631- 639.

Mbhele, Z.M., Sakmane M.G., van Sittert C.G.C.E., Nedeljkovic J.M., Djokovic V. and Luyt A.S. (2003). Fabrication and Characterization of Silver-Polyvinyl Alcohol Nanocomposites. *Chemistry of Materials* 15: 5019-5024.

Min, S., Wang F. and Han Y. (2007). An investigation on synthesis and photocatalytic activity of polyaniline sensitized nanocrystalline TiO2 composites. *Journal of Materials Science* 42: 9966-9972.

Neppolian, B., Choi H.C., Sakthivel S., Arabindoo B., and Murugesan V. (2002). Solar /UV-induced photo catalytic degradation of three commercial textile dyes. *Journal of Hazardous Materials* 89: 303 - 3 17.

Niu, Z., Yang Z., Hu Z., Lu Y., Han C.C. (2003). Polyaniline-Silica Composite Conductive Capsules and Hollow Spheres. *Advanced Functional Materials* 13: 949-954.

Olad, A. and Nosrati R. (2011). Preparation, characterization, and photocatalytic activity of polyaniline/ZnO nanocomposite. *Research on Chemical Intermediates* 38(2): 326-336.

Parida, K.M., Dash S.S. and Das D.P. (2006). Physico-chemical characterization and hotocatalytic activity of zinc oxide prepared by various methods. *Journal of Colloid and Interface Science* 298: 787-793.

Pouget, J.P., Hsu C.H., MacDiarmid A.G. and Epstein A.J. (1995). Structural investigation of metallic PAN-CSA and some of its derivatives. *Synthetic Metals* 69: 119-120.

Poulios, I. and Aetopoulou I. (1999). Photocatalytic Decomposition of Commercial Azo Dye Reactive Orange. *Environmental Technology* 20: 479.

Rao, V.S., Rao K.S., Rao M.N. and Bora1 U. S. (2011). Studies on the surface characterisation of newly prepared activated kaza's carbons. *Asian Journal Of Biochemical and Pharmaceutical Research* 2(1): 567-84.

Rashed, M.N. and El-Amin A.A. (2007). Photocatalytic degradation of methyl orange in aqueous TiO_2 under different solar irradiation sources. *International Journal of Physical Sciences* 2(3): 073-081.

Sakthivela, S.B., Neppolianb M.V., Shankarb B., Arabindoob M., Palanichamyb V. and Murugesanb V. (2003). Solar photocatalytic degradation of azo dye: comparison of photocatalytic efficiency of ZnO and TiO_2, *Solar Energy* Materials and *Solar Cells* 77: 65-82.

Sedenkova I., Trchova M. and Stejskal J. (2008). The thermal degradation of polyanilinefilms prepared in solutions and weak acids and in water-FTIR and Raman spectroscopic studies. *Polymer Degradation and Stability* 93: 2147-2157.

Shaheen, S.E., Brabec C.J., Padinger F., Fromherz T., Hummelen J.C. and Sarıçiftçi N.S. (2001). 2.5 % Efficient Organic Plastic Solar Cells. *Applied Physics Letters* 78: 841-843.

Sharma, B.K., Gupta A.K., Khare N., Dhawan S.K. and Gupta H.C. (2009). Synthesis and characterization of polyaniline-ZnO composite and its dielectric behavior. *Synthetic Metals* 159: 391-395.

Silva, R.F. and Zaniquelli M.E.D. (2002). Morphology of nanometric size particulate aluminium-doped zinc oxide films. *Colloids and Surfaces*A 551: 198.

Somani, P.R., marimuthu R., Mulik U.P., Sainkar S.R., Amelnerkar D.P. (1999). High piezoresistivity and its origin in conducting polyaniline/TiO_2 composites. *Synthetic Metals* 106: 45-52.

Wang, X., Li Y., Zhao Y., Liu J., Saide T. and Feng W. (2010). Synthesis of PANI nanostructures with various morphologies from fibers to micromats to disks doped with salicylic acid. *Synthetic Metals* 160: 2008-2014.

Wong, C.C. and Chu W. (2003). The direct photolysis and photocatalytic degradation of alachlor at different TiO2 and UV sources. *Chemosphere* 50: 981-987.

Xu, J.F., Lin J.Y. , Tang S.H. and Duy W. (1998). Preparation of ZnS nanoparticles by ultrasonic radiation method. *Applied Physics A,* 66(6): 639−641.

Xu, Z.X.,. Roy V.A.L, Stallinga P., Muccini M., Toffanin S., Xiang H.F. and Che C.M. 2007. Nanocomposite field effect transistors based on zinc oxide/polymer blends *Applied Physics Letters* 90: 223509/1-223509/3.

Zhu, C., Wang L., Kong L., Yang X., Zheng S., Chen F., Maizhi F. and Zong H. (2000). Photocatalytic degradation of azo dyes by supported TiO_2 + UV in aqueous solution. *Chemosphere* 41: 303-309.